

# Deposition of tin oxide, iridium and iridium oxide films by metal-organic chemical vapor deposition for electrochemical wastewater treatment

Songsak Klamklang · Hugues Vergnes ·  
François Senocq · Kejvalee Pruksathorn ·  
Patrick Duverneuil · Somsak Damronglerd

Received: 1 December 2008 / Accepted: 9 July 2009 / Published online: 28 July 2009  
© Springer Science+Business Media B.V. 2009

**Abstract** In this research, the specific electrodes were prepared by metal-organic chemical vapor deposition (MOCVD) in a hot-wall CVD reactor with the presence of  $O_2$  under reduced pressure. The Ir protective layer was deposited by using (Methylcyclopentadienyl) (1,5-cyclo-octadiene) iridium (I), (MeCp)Ir(COD), as precursor. Tetraethyltin (TET) was used as precursor for the deposition of  $SnO_2$  active layer. The optimum condition for Ir film deposition was at 300 °C, 125 of  $O_2$ /(MeCp)Ir(COD) molar ratio and 12 Torr of total pressure. While that of  $SnO_2$  active layer was at 380 °C, 1200 of  $O_2$ /TET molar ratio and 15 Torr of total pressure. The prepared  $SnO_2$ /Ir/Ti electrodes were tested for anodic oxidation of organic pollutant in a simple three-electrode electrochemical reactor using oxalic acid as model solution. The electrochemical experiments indicate that more than 80% of organic pollutant was removed after 2.1 Ah/L of charge has been applied. The kinetic investigation gives a two-step process for organic pollutant degradation, the kinetic was zero-order and first-order with respect to TOC of model solution for high and low TOC concentrations, respectively.

**Keywords** Wastewater treatment · Electrochemical oxidation · Specific electrode · MOCVD · Thin film coating

## 1 Introduction

Electrochemistry is a clean, versatile and powerful tool for the destruction of organic pollutants in water and its applications were used in several areas [1–7]. Electrochemical oxidation of organic compounds in aqueous solution is an anodic process occurring in the potential region of water discharge to produce oxygen. Two different pathways are described in the literatures for the anode oxidation of undesired organic pollutants [2, 3]. In fact, the toxic non-biodegradable pollutants are able to transform into biodegradable organics by electrochemical conversion, but biological treatment is still required after the electrochemical conversion [3]. Electrochemical combustion method completely oxidizes the organic pollutants to  $CO_2$  by hydroxyl radicals. In this case, the electrode material must have high electrocatalytic activity towards the electrochemical oxidation of organics to  $CO_2$  and  $H_2O$  [3].

The active coating materials of electrodes are essential for pollutants degradation in electrochemical combustion process. It could point the project to be benefit or insolvent. Comninellis and Vercesi [4] found that the  $Ta_2O_5$ -doped  $IrO_2$  had given the highest service life. Nevertheless, the mechanism of electrochemical oxidation of organic pollutant on  $IrO_2$  electrode was selective oxidation that presented the lower efficiency for organic pollutants removal. In recent years, there are some publications on the application of diamond electrode for wastewater treatment [8–17]. However, the application of diamond electrode for organic pollutant degradation is still limited by the cost of diamond electrode and its brittleness.  $SnO_2$  is one of the best candidates for removal of organic

S. Klamklang · H. Vergnes (✉) · P. Duverneuil  
Laboratoire de Génie Chimique, Site Basso Cambo, 5 rue Paulin  
Talabot, 31106 Toulouse Cedex 01, France  
e-mail: hugues.vergnes@ensiacet.fr

S. Klamklang · K. Pruksathorn · S. Damronglerd  
Department of Chemical Technology, Faculty of Science,  
Chulalongkorn University, Phayathai Rd., Phatumwan,  
Bangkok 10330, Thailand

F. Senocq  
Centre Interuniversitaire de Recherche et d'Ingénierie des  
Matériaux, 118, Route de Narbonne, 31077 Toulouse Cedex 04,  
France

pollutants from wastewater by electrochemical oxidation [1–5]. There are a variety of methods suitable for preparation of SnO<sub>2</sub> layer such as reactive sputtering, sol–gel, dip coating, spray-pyrolysis and chemical vapor deposition [2].

Ir is a noble metal with a small unit cell dimension, owing to this property; Ir acts as a good diffusion barrier and has a great interest as protective coating due to its good resistance against corrosion and oxidation [18]. Ir is also a valve metal well know to have conducting oxide.

Chemical vapor deposition (CVD) is very attractive process for electrode coating, due to its good coverage and uniform deposition. This advantage should improve the service life of the electrode as it avoids the oxidation of the substrate by the diffusion of electrolyte via the cracks resulting from the shrinkage during the annealing step found in some coatings prepared by sol–gel or other thermal deposition [7, 19]. Furthermore, the using of metal-organic chemical vapor deposition (MOCVD) permits significant decreasing of the deposition temperature and high purity of deposited layer.

In this paper, the preparation and characterization of SnO<sub>2</sub> electrodes with Ir protective layer for organic pollutant degradation in electrochemical oxidation process by MOCVD on the various substrates were reported. The coatings were characterized by XRD and SEM. The suitable electrodes were tested for pollutant removal efficiency.

## 2 Experimental

### 2.1 Materials

(Methylcyclopentadienyl) (1,5-cyclooctadiene) iridium (I), 99% w/w was supplied by Strem Chemicals Inc., Tetraethyltin 97% w/w was supplied by Aldrich Chemical Co., Inc. Oxalic acid 98% w/w, HCl 35% v/v, HF 40% v/v and Acetone 99% v/v were supplied by BDH Chemicals Inc. Si wafer was electronic grade with orientation of 110. The TaC was kindness supplied by Prof. Dr. Pierre Chamelot that was prepared by electrochemical technique [20].

### 2.2 Pretreatment of substrates

The Si wafers (8 × 10 mm) were degreased in hot acetone, rinsed with de-ionized water and dried by compressed air. Ti sheets (8 × 30 mm) were etched in hot 35% HCl for 1 h, rinsed by de-ionized water and dried by compressed air. Ta substrates (8 × 30 mm) were etched in 40% HF from 1 min to 24 h, rinsed by de-ionized water and dried by compressed air. To remove the free carbon on the TaC/Ta surface, it was polished by stainless steel rotating brush and etched in 40% HF for 1 h. Then, it was rinsed by de-ionized water and dried by compressed air.

### 2.3 Deposition of Ir protective layer

To improve the service life of specific SnO<sub>2</sub> electrode, the Ti substrate needs to be coated with a protective layer. The Ir deposition was studied in horizontal hot-wall CVD reactor with 1.2 cm internal diameter and 15 cm isothermal zone, the apparatus being represented in Fig. 1. (MeCp)Ir(COD) was used as organo-iridium precursor. The deposition temperature was in the range of 300–350 °C and 12 Torr of total pressure. The (MeCp)Ir(COD) was contained in the glass bubbler at 85 °C. This temperature allows the precursors to be melted and improved its transport properties. Helium and oxygen were used as carrier and co-reactive gases, respectively. The gas flow rate was monitored and controlled by mass-flow control and the total pressure was automatically controlled using an absolute pressure gauge coupled to the throttle valve system.

### 2.4 Preparation of SnO<sub>2</sub> active coating

The SnO<sub>2</sub> film was grown on the pretreated substrates in the same CVD apparatus used for Ir deposition. TET was used as tin source precursor. Helium and oxygen were used as carrier and co-reactive gases, respectively. TET was contained in stainless steel bubbler at 2 °C. The depositions were performed at 380 °C and 15 Torr of total pressure.

### 2.5 Sample characterization

The surface morphology and microstructure of the coatings were characterized by X-ray diffraction (Seiffert XRD 3000TT, Cu K $\alpha$ ) and scanning electron microscope (Jeol JSM-6400). Surface roughness has been determined by

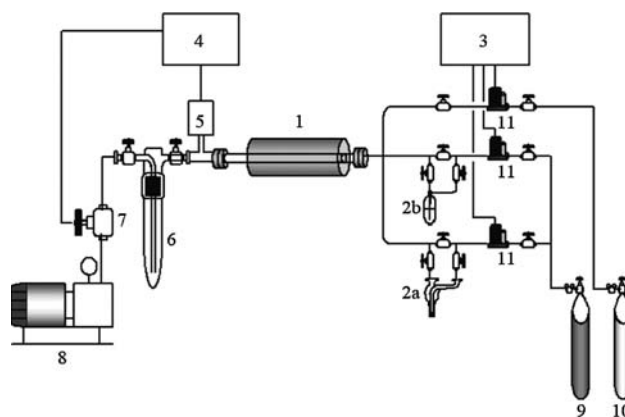


**Fig. 1** MOCVD apparatus: (1) Hot-wall CVD reactor. (2a) 1st bubbler for (MeCp)Ir(COD). (2b) 2nd bubbler for TET. (3) Gas flow controller. (4) Pressure controller. (5) Pressure gauge. (6) Cold trap. (7) Throttle valve. (8) Vacuum pump. (9) He tank. (10) O<sub>2</sub> tank. (11) Mass-flow controller

profilometry (Tencor P2). The relative average deposited films growth rate was determined by weight measurement using six digits balance (Sartorius ME36S).

## 2.6 Electrochemical measurement

The electrochemical characterization was performed in a conventional three-electrode electrochemical reactor with 2-active surfaces of  $0.8 \times 2.0 \text{ cm}^2$   $\text{SnO}_2/\text{Ir}/\text{Ti}$  flat electrode, 1 cm of anode–cathode distance and 15 mL of its capacity. The prepared electrodes were used as anode, the 316L stainless steel was used as cathode and the saturated calomel was used as reference electrode. The kinetic was studied at 30 °C and 300 rpm of mixing speed using 2-cm magnetic stirrer. The electrical current was supplied using constant current mode by potentiostat (Autolab PGSTAT 100). The pollutant removal efficiency was investigated by using oxalic acid as model solution and determined from the total organic carbon (TOC). TOC was determined by Shimadzu TOC-5050A analyzer.

## 3 Results and discussion

### 3.1 Treatment of substrates

To improve the surface roughness of substrates for better adhesion of deposited films, the substrates need to be etched by the appropriating acid. In case of Ta substrate,

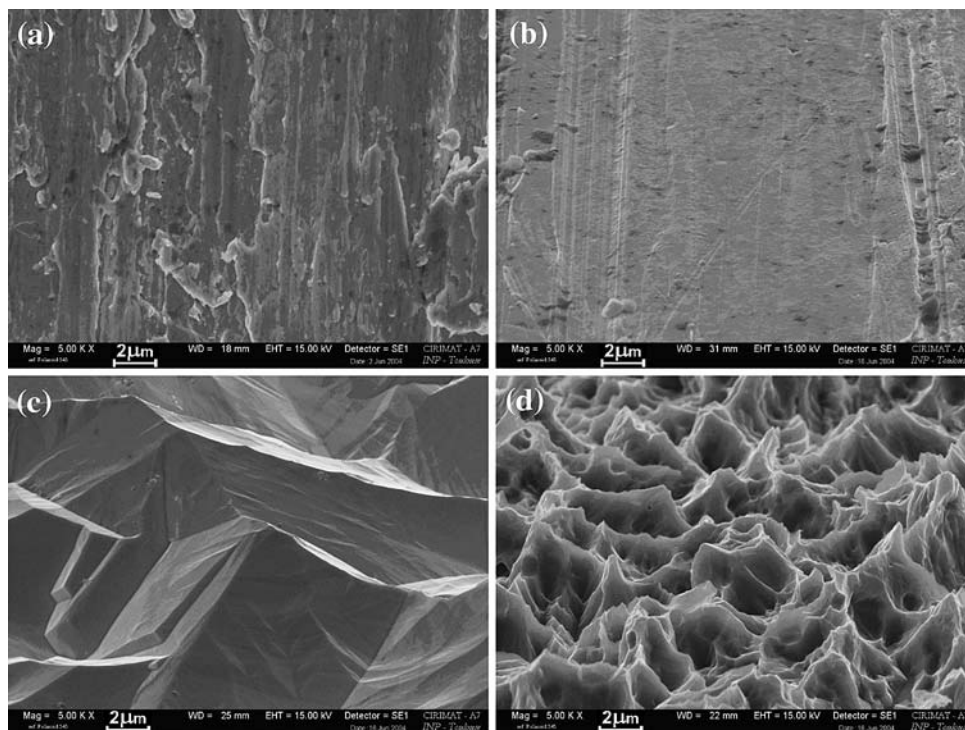
the 40% HF was used as etching reagent. After etching, the average surface roughness of Ta substrates was increased. The Ta surface roughness progressed slowly comparing with Ti substrates etched by hot-HCl for 1 h. Although, Ta substrate was etched by stronger acid as HF, nevertheless the Ta surface roughness was still smaller than Ti surface because the chemical stability of Ta is much higher than that of Ti substrate. The average surface roughness of 1 h hot-HCl etched Ti was 414 nm, while the average surface roughness of Ta substrates at various etching time is less than 300 nm. The increasing surface area was confirmed by the SEM observation as shown in Fig. 2.

### 3.2 Deposition of Ir protective layer

Deposition of Ir film by using  $(\text{MeCp})\text{Ir}(\text{COD})$  as precursor for MOCVD could be operated in various conditions [18, 21]. In this work, the deposition of Ir film with the presence of  $\text{O}_2$  was investigated. It was found that the deposition of Ir film was strongly affected by deposition temperature and oxygen content in feed vapor mixture.

At high  $\text{O}_2/(\text{MeCp})\text{Ir}(\text{COD})$  molar ratio in feed gas mixture, the increasing deposition temperature from 300 to 325 and 350 °C has a significant affect on the deposition area of Ir film. The deposition area of Ir film was decreased from 13 to 11 and 9.75 cm from the entrance of the reactor, respectively.  $(\text{MeCp})\text{Ir}(\text{COD})$  was completely decomposed and yield of the Ir deposited film in the reactor was nearly 100%. However, the Ir film was deposited only at the

**Fig. 2** Scanning electron micrographs of some substrates: **a** Ta without etching. **b** Ta with 1 h etching. **c** Ta with 24 h etching. **d** Ti with 1 h etching



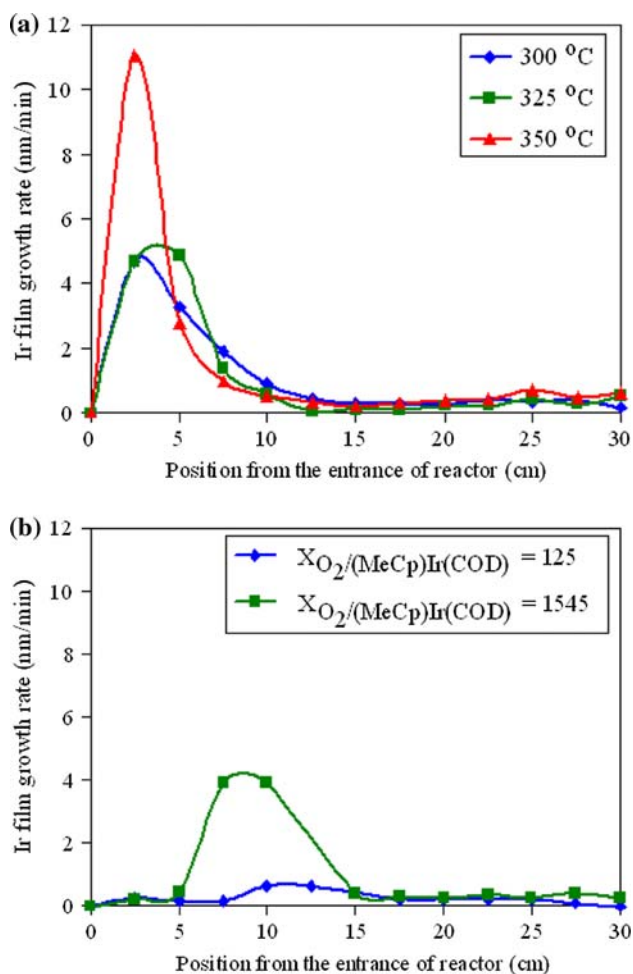


**Fig. 3** Effect of deposition parameters on Ir film growth rate: **a** Effect of deposition temperature on Ir film growth rate at 12 Torr and  $O_2/(\text{MeCp})\text{Ir}(\text{COD})$  molar ratio of  $1491 \pm 89$ . **b** Effect of oxygen molar ratio on Ir film growth rate at 300 °C and 12 Torr

entrance of the reactor because the system had very high reactivity when oxygen content was high. It is in good agreement with some results shown in Fig. 3a: the growth rate of Ir film was very high at a few centimeters near the entrance of the reactor. So, the precursor reacted with

co-reactive gas and it was consumed immediately a few centimeters from the entrance.

In contrast at low  $O_2/(\text{MeCp})\text{Ir}(\text{COD})$  molar ratio of 125, the reactivity of the system was decreased by reducing  $O_2/(\text{MeCp})\text{Ir}(\text{COD})$  molar ratio. In this case, the Ir film deposited uniformly over several centimeters distance through the reactor. Figure 3b shows that the growth rate increased to the 10 cm from the entrance before decreasing rapidly downstream.

Figure 4 represents the SEM images of Ir film on Si wafer and hot-HCl treated Ti substrate. The micrographs present very smooth, homogeneous and good coverage deposition of Ir film. The Ir deposition also has very high purity. It could be confirmed by the XRD spectra in Fig. 5. From these results, we could say that it is possible to prepare an Ir protective layer before  $\text{SnO}_2$  coating.

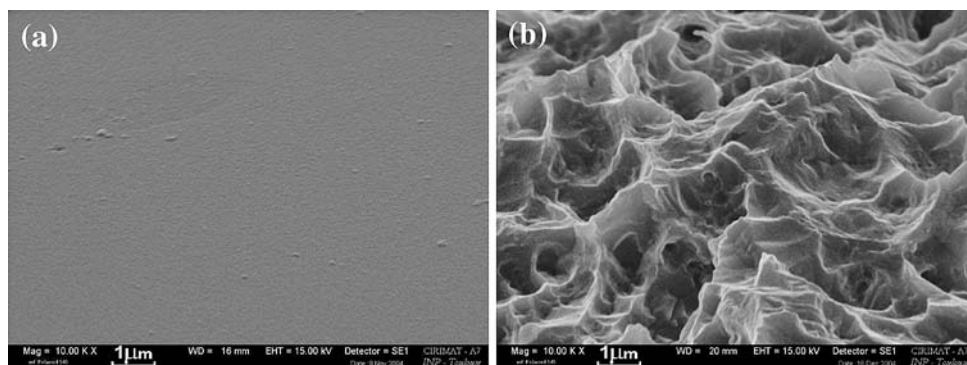
From these results it could be concluded that the Ir film deposited at 300 °C with total pressure of 12 Torr and  $O_2/(\text{MeCp})\text{Ir}(\text{COD})$  molar ratio of 125 is suitable to be used as the protective layer for specific electrode.

### 3.3 Deposition of $\text{SnO}_2$ active coating

Figure 6 presents the effect of feed vapor composition on the  $\text{SnO}_2$  deposition, it was found that increasing  $O_2/\text{TET}$  molar ratio from 300 to 1,200, the both growth rates of  $\text{SnO}_2$  film were quite similar in first 10 cm from the entrance. Nevertheless, in isothermal zone (after first 10 cm), the  $O_2/\text{TET}$  molar ratio of 300 represented the higher growth rate of  $\text{SnO}_2$  film. It may be caused at the first 10 cm, the system temperature was still low and the internal energy of TET precursor was not enough to react with mixed oxygen. However, after system reached to the isothermal zone, the effect of TET precursor in feed vapor was outstanding. The growth rate of  $\text{SnO}_2$  film was a function of TET concentration in feed gas composition. Similar results were found in deposition of Ir film by MOCVD in previous report [22].

The XRD spectra in Fig. 7 presents increasing TET concentration in feed gas mixture has no influence on

**Fig. 4** Scanning electron micrographs of Ir film: **a** Ir film over Si wafer. **b** Ir film over 1 h hot-HCl treated Ti substrate





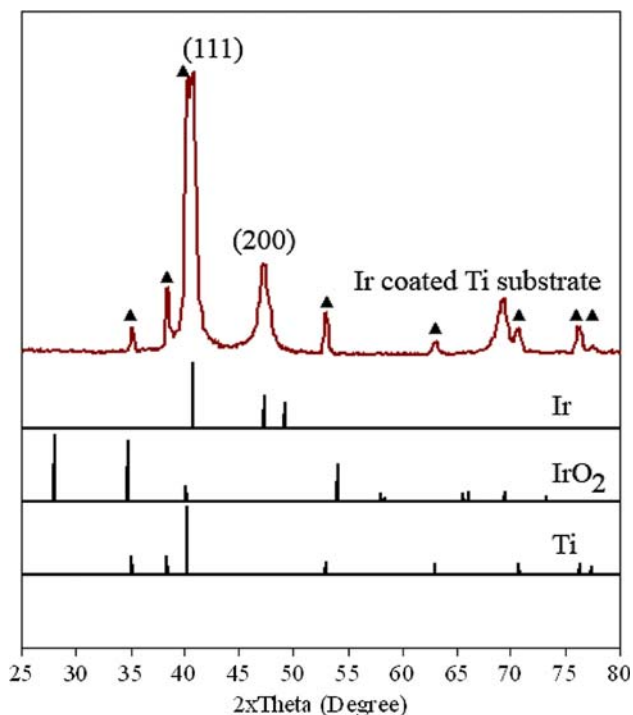


Fig. 5 X-ray diffraction of Ir coated Ti substrate (triangle) substrate

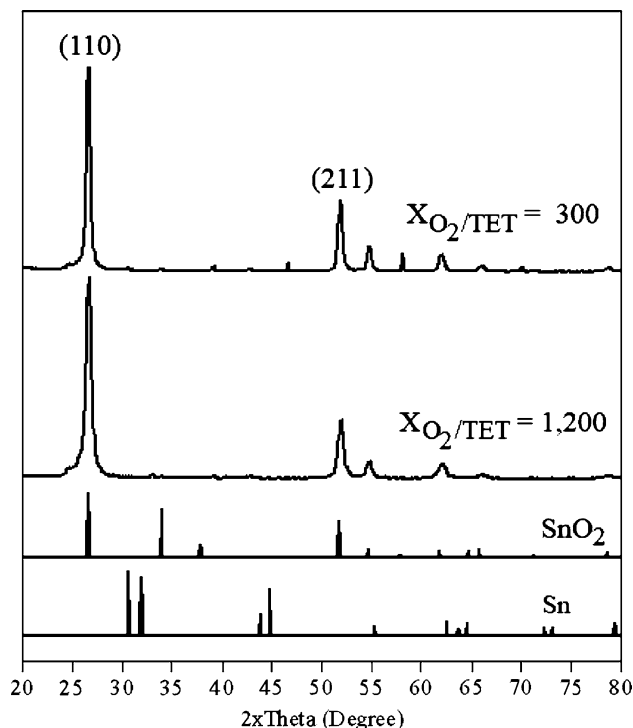


Fig. 7 X-ray diffraction of SnO<sub>2</sub> film over Si wafer at 380 °C and 15 Torr

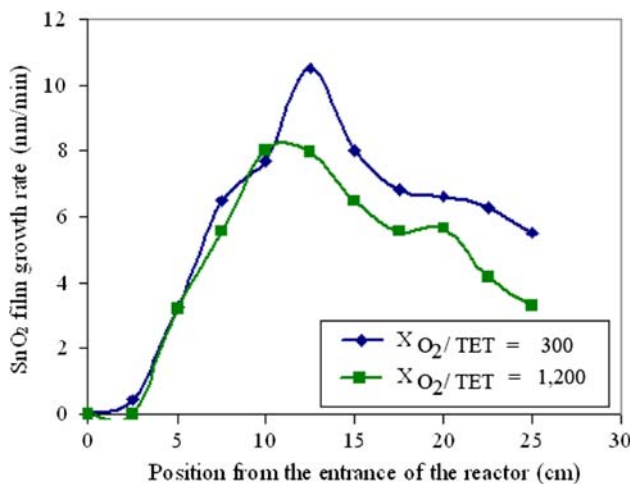


Fig. 6 Effect of feed gas composition on SnO<sub>2</sub> film growth rate at 380 °C and 15 Torr

the microstructure of SnO<sub>2</sub> film. The SnO<sub>2</sub> film has nearly similar XRD spectra in both 300 and 1,200 O<sub>2</sub>/TET ratio.

From previous results for which SnO<sub>2</sub> was deposited on Si wafer, it was found that the growth rate of SnO<sub>2</sub> film was smooth and uniform between 17.5 and 22.5 cm from the entrance of the reactor. So, in the preparation of useful electrode, the substrate was placed between 17.5 and 20.5 cm from the entrance and the dashed line in Fig. 8 is represented the placement area of substrate in SnO<sub>2</sub> film

deposition. To measure the growth rate profile and to be sure that the system was similar to the previous one, the Si wafers were still placed on the other point in the reactor as in previous runs.

The effect of substrate on SnO<sub>2</sub> film growth rate was presented in Fig. 8. In placement area of actual substrates, the growth rate of SnO<sub>2</sub> film was slightly increased when substituted with Si wafer at 1 min and 1 h HF-treated Ta.

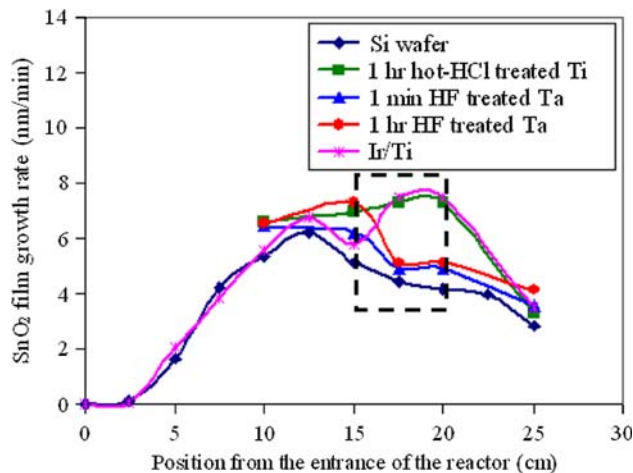
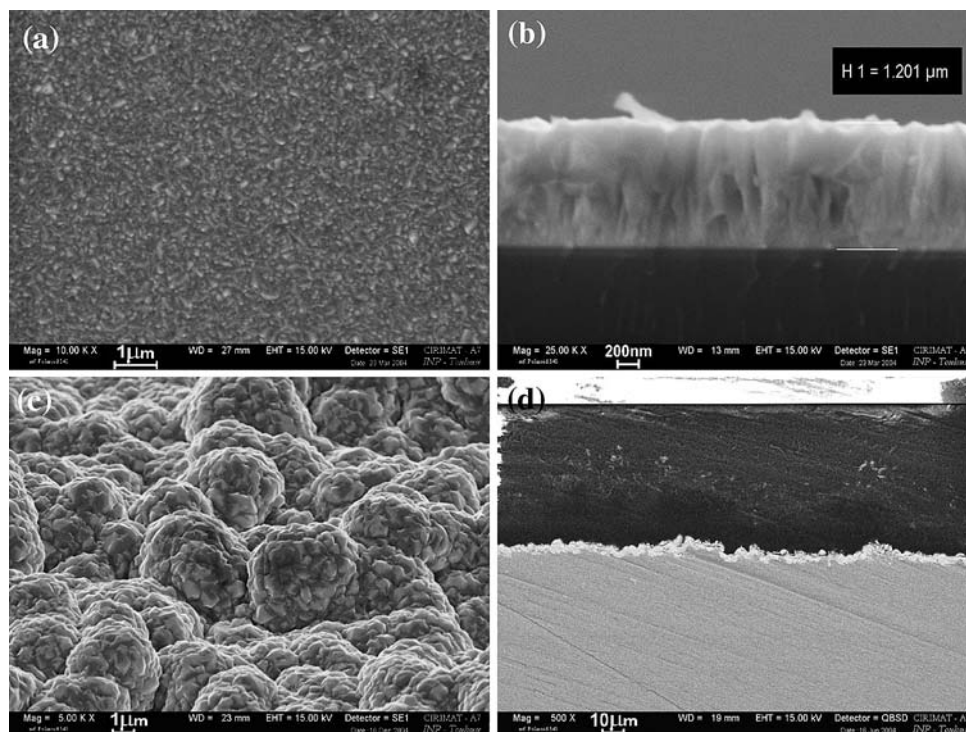


Fig. 8 Effect of substrate on SnO<sub>2</sub> film growth rate at 380 °C and 15 Torr

**Fig. 9** Surface and cross-sectional microstructure of SnO<sub>2</sub> film over various substrates: **a–b** Si wafer, **c–d** Ir/Ti



After replacing silicone wafer with HCl-treated Ti and Ir coated Ti substrate, the growth rate abruptly and drastically increased. It seems as if the boost was a direct result from the substitution; however, differences in roughness of the substrate were not considered. Rougher surface allowed the HCl-treated Ti and Ir coated Ti substrate to stick to the groves causing the film to be more important. After treating with HCl acid, the treated Ti possessed a much rougher surface as presented in Fig. 4, which led to a higher specific area in the same geometrical dimension. Therefore, the high SnO<sub>2</sub> film growth rate was presented at the substitution of Si wafer by HCl-treated Ti and Ir coated Ti substrate when determined the SnO<sub>2</sub> film growth rate by its weight.

Figure 9 represents the surface and cross-section pictures of SnO<sub>2</sub> film on Si wafer and Ir coated Ti substrate. The deposited SnO<sub>2</sub> film over Si wafer has dense, smooth and homogeneous microstructure. In the case of Ir coated Ti substrate, the microstructure of SnO<sub>2</sub> film was still dense and homogeneous. Furthermore, it also presents the good coverage deposition on the high surface roughness of Ir coated Ti substrate. This last point shows the interest of the pre-treatment in order to improve the adhesion of the layer and also to increase the electrodes specific surface and so theirs catalytic activities.

From the results, it could be concluded that the suitable SnO<sub>2</sub> active coating for use as anode organic pollutant degradation was deposited at 380 °C, 15 Torr of total pressure and 1,200 of O<sub>2</sub>/TET molar ratio.

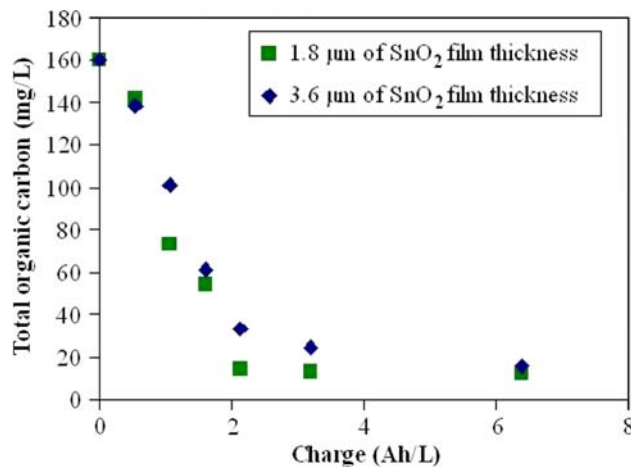


**Fig. 10** Variation of TOC of electrolyze during mineralization using SnO<sub>2</sub>/Ir/Ti, electrode surface area of 3.2 cm<sup>2</sup> and current density of 5 mA/cm<sup>2</sup>

### 3.4 Electrochemical characterization

It is well known that SnO<sub>2</sub> electrode is powerful for organic pollutant destruction by anodic oxidation [3, 19, 23, 24]. Figure 10 represents the removal of oxalic acid by specific SnO<sub>2</sub>/Ir/Ti electrode with two different SnO<sub>2</sub> film thicknesses. The results showed that the SnO<sub>2</sub> thickness has not a great effect on the oxalic acid destruction. It may be because the production of adsorbed hydroxyl radicals occurred only at the surface of electrode. However, Duverneuil et al. [19] proposed that taking account the life

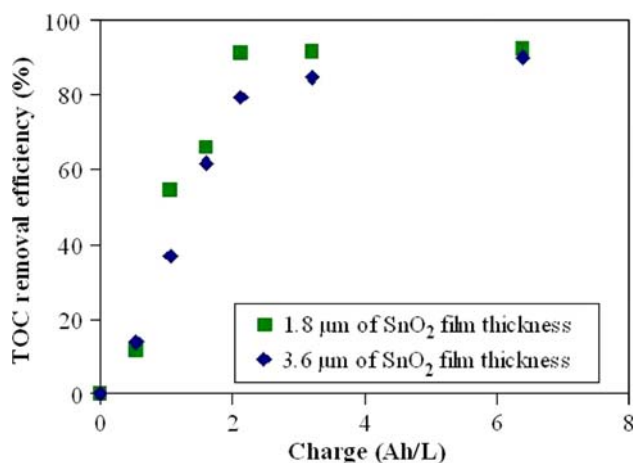


**Fig. 11** TOC removal efficiency by using SnO<sub>2</sub>/Ir/Ti, electrode surface area of 3.2 cm<sup>2</sup> and current density of 5 mA/cm<sup>2</sup>

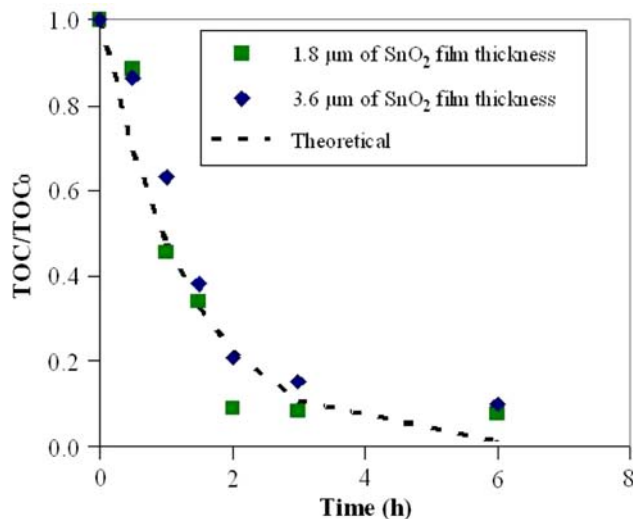


**Fig. 12** Dimensionless concentration variation of TOC during mineralization using SnO<sub>2</sub>/Ir/Ti, electrode surface area of 3.2 cm<sup>2</sup> and current density of 5 mA/cm<sup>2</sup>

time of the electrode, the optimum SnO<sub>2</sub> thickness is 2–5 microns because microcracks have been observed in thicker SnO<sub>2</sub> film due to the thermal stress in SnO<sub>2</sub> film during the deposition process.

Figures 10 and 11 present the decreasing of the TOC concentration and TOC removal efficiency versus time. More than 80% of TOC has been removed up to 2 h or 2.1 Ah/L from the initial concentration (160.4 mg/L of TOC). Then the TOC of model solution decreases only slightly. In case of rate limiting by mass transfer, TOC concentration should follow exponential decline;

$$TOC = TOC_0 \exp(-t/\tau)$$

with time constant,  $\tau$  is defined as;

$$\tau = \frac{V}{k_d \cdot S}$$

Considering the value of the volume ( $V = 15 \text{ cm}^3$ ) and the area of the anode ( $S = 3.2 \text{ cm}^2$ ), the average mass transfer coefficient ( $k_d$ ) is 0.0018 cm/s that agreed with value of 0.002 cm/s as found by Weiss et al. [13]. Figure 12 presents comparison of the experimental dimensionless concentration of TOC obtained for the two different SnO<sub>2</sub> film thicknesses versus theoretical curve as function of time. Figure 12 shows that the theoretical curve well fit with the experimental data, therefore it could be concluded that the oxalic acid degradation is mass transfer limited.

Increasing current density from 5 to 10 mA/cm<sup>2</sup>, leads to less degradation rate of oxalic acid by electrochemical oxidation. This behavior is characteristic of mass transfer-controlled processes [25]. In such systems, the increase of current density can not increase the organic removal efficiency at the electrode, but only favors oxygen evolution as the anodic side reaction which hides the electrode and prevents contact between hydroxyl radicals and organic pollutants. When the system does not generate only adsorbed hydroxyl radicals or other active oxygen, the decrease of organic pollutant removal efficiency is observed.

In the case of SnO<sub>2</sub>/TaC/Ta, the SnO<sub>2</sub> layer passivation was observed after a few minutes in electrochemical characterization which was attributed to some free carbon that remained on TaC surface.

#### 4 Conclusions

The specific SnO<sub>2</sub>/Ir/Ti prepared by metal-organic chemical vapor deposition is powerful for the degradation of organic pollutant presented in wastewater by electrochemical oxidation. Ir film deposited at 300 °C, 12 Torr of total pressure and 125 of O<sub>2</sub>/(MeCp)Ir(COD) molar ratio is suitable to be used as the protective layer for specific electrode. The useful SnO<sub>2</sub> active coating for using as anode organic pollutant degradation was deposited at 380 °C, 15 Torr of total pressure and 1,200 of O<sub>2</sub>/TET molar ratio. The oxalic acid degradation kinetic was mass transfer limitation and the mass transfer coefficient of 0.0018 cm/s was determined. However, the electrodes service life measurement is still running.

**Acknowledgements** The authors gratefully acknowledge the Royal Golden Jubilee Ph.D. Program of Thailand Research Fund for the financial support during the Ph.D. of Mr. Songsak Klamklang (PHD/0200/2544) and the French Embassy in Thailand for financial support during research work in France. Prof. Dr. Pierre Chamelot for kindness supply of TaC substrates.

## References

1. Chen X, Chen G, Yue PL (2000) *Sep Purif Technol* 19:65
2. Grimm J, Bessarabov D, Maier W, Storck S, Sanderson RD (1998) *Desalination* 115:295
3. Comninellis Ch (1994) *Electrochim Acta* 39:1857
4. Comninellis Ch, Vercesi GP (1991) *J Appl Electrochem* 21:335
5. Stucki S, Kötzt R, Carcer B, Suter W (1991) *J Appl Electrochem* 21:99
6. Wu Z, Cong Y, Zhou M, Ye Q, Tan T (2002) *Korean J Chem Eng* 19:866
7. Sathish M, Viswanath RP (2005) *Korean J Chem Eng* 22:358
8. Diniz AV, Ferreira NG, Corat EJ, Trava-Airolo VJ (2003) *Diam Relat Mater* 12:577
9. Panizza M, Cerisola G (2005) *Electrochim Acta* 51:191
10. Fernandes A, Morão A, Magrinho M, Lopes A, Gonçalves I (2004) *Dye Pigment* 61:287
11. Morão A, Lopes A, Pessoa de Amorim MT, Gonçalves I (2004) *Electrochim Acta* 49:1587
12. Lissens G, Pieters J, Verhaege M, Pinoy L, Verstraete W (2003) *Electrochim Acta* 48:1655
13. Weiss E, Groenen-Serrano K, Savall A, Comninellis Ch (2007) *J Appl Electrochem* 37:41
14. Weiss E, Groenen-Serrano K, Savall A (2008) *J Appl Electrochem* 38:329
15. Siné G, Duo I, El Roustom B, Fóti G, Comninellis Ch (2006) *J Appl Electrochem* 36:847
16. Ammar S, Abdelhedi R, Flox C, Arias C, Brillas E (2006) *Environ Chem Lett* 4:229
17. Martínez-Huitle CA, Ferro S, De Battisti A (2005) *J Appl Electrochem* 35:1087
18. Maury F, Senocq F (2003) *Surf Coat Technol* 163–164:208
19. Duverneuil P, Maury F, Pebere N, Senocq F, Vergnes H (2002) *Surf Coat Technol* 151–152:9
20. Massot L, Chamelot P, Taxil P (2006) *J Alloys Compd* 424:199
21. Hoke JB, Stern EW, Murray HH (1991) *J Mater Chem* 1:551
22. Amjoud MB, Maury F, Soukane S, Duverneuil P (1998) *Surf Coat Technol* 100–101:169
23. Vercesi G, Rolewicz J, Comninellis Ch, Hinder J (1991) *Thermochim Acta* 176:31
24. Comninellis Ch, Nerini A (1995) *J Appl Electrochem* 25:23
25. Kesselman JM, Weres O, Lewis NS, Hoffmann MR (1997) *J Phys Chem B* 101:2637